Journal of Molecular Catalysis A: Chemical 318 (2010) 101–105

Contents lists available at ScienceDirect

Journal of Molecular Catalysis A: Chemical

journal homepage: www.elsevier.com/locate/molcata

Effect of N atoms in the backbone of metal phthalocyanine derivatives on their catalytic activity to lithium battery

Zhanwei Xu[a,b], Guoxiang Zhang[a], Zeyuan Cao[b], Jianshe Zhao[a,*], Hejun Li[b]

[a] Key Laboratory of Synthetic and Natural Functional Molecule Chemistry of Ministry of Education, Department of Chemistry, Northwest University, Xi'an 710069, PR China
[b] C/C Composites Research Center, National Key Laboratory of Thermostructure Composite Materials, Northwestern Polytechnical University, Xi'an 710072, PR China

ARTICLE INFO

Article history:
Received 15 September 2009
Received in revised form
17 November 2009
Accepted 22 November 2009
Available online 26 November 2009

Keywords:
Phthalocyanine
Electron transfer
Catalytic active site
Thionyl chloride

ABSTRACT

Metal phthalocyanine (MPc, M = Mn^{2+}, Fe^{2+}, Co^{2+}, Ni^{2+} and Cu^{2+}), metal tetrapyridinoporphyrazine, and metal tetrapyrazinoporphyrazine are synthesized by microwave reaction and characterized by elemental analyzer, IR spectroscopy and UV–vis spectroscopy. The catalytic activity of MPc derivatives to Li/$SOCl_2$ battery is evaluated by the relative discharge energy of the battery whose electrolyte contains the compounds. The discharge energy of Li/$SOCl_2$ battery catalyzed by MPc is approximately 0–61% higher than that of Li/$SOCl_2$ battery in the absence of compounds, depending on the central metal ion. To the same central metal ion, the discharge energy of Li/$SOCl_2$ battery catalyzed by MTAP is approximately 60% higher than that by MPc. The discharge energy of Li/$SOCl_2$ battery in which $SOCl_2$ contains MPTpz is approximately 17–19% higher than that of the battery in the absence of compounds, and almost independent of central metal ions. It shows a correlation existing between the structure and the catalytic active sites of MPc derivatives. The double active site model is proposed to interpret the results.

1. Introduction

Metal phthalocyanine (MPc) derivatives are conjugated macromolecules, and have unique plane structure, excellent electronic property, which attracts much interest in the fields of solar energy conversion [1,2], semiconductor [3–5], and catalysis [6–10].

On the other hand, due to the excellent characteristics, such as high-specific energy, high-rate capability, long shelf-life and wide range operational temperature (−55 to 85 °C), lithium (Li/$SOCl_2$) battery causes much focus. However, one of limitations of present Li/$SOCl_2$ battery is that its energy in practice is much lower than that in the theory. In addition, Li/$SOCl_2$ battery is mainly used as the primary battery or reserved battery to supply the power to the instrument operated in long time and in the rough-weather research, which makes the improvement of the practical energy of Li/$SOCl_2$ battery increasingly urgent. Extensive works have been done to promote the practical energy of Li/$SOCl_2$ battery [11–21]. Among these works, using macromolecular compounds, especially metal phthalocyanine compounds acting as catalyst attracted much interest [14–18]. The catalytic activity is predominantly controlled by the catalytic active sites of the compounds and their catalytic activity. Many works associated with the effects of central metal ions and substitutes of MPc derivative to catalytic activity have been reported, however, to the best of our knowledge, no work has demonstrated the number of the active sites of metal phthalocyanine compounds and their catalytic activity. It is the requirement that the compound used as catalyst of the battery is readily both oxidizable and reducible [22]. The N atoms in the outer ring of MPc derivatives strongly affect the property of metal phthalocyanines [23–26]. In this paper we focus on the analysis of the N atoms in the backbone of the ligands on the catalytic activity of the metal phthalocyanine derivatives.

2. Experimental

In order to show the effect of N atoms in the backbone of MPc derivatives on their catalytic activity to lithium battery, MPc (M = Mn^{2+}, Fe^{2+}, Co^{2+}, Ni^{2+} and Cu^{2+}), metal tetrapyridinoporphyrazine (MTAP) and metal tetrapyrazinoporphyrazine (MPTpz) with 4, 8 and 12 N atoms in the outer ring respectively (the chemical structure of MPc, MTAP and MPTpz is shown in Fig. 1) are synthesized and used as catalysts to Li/$SOCl_2$ battery. Elemental analysis (carbon, hydrogen, nitrogen) is performed on a Germany VarioEL III CHNOS analyzer. IR spectra of the products are measured using a Germany EQUINOX 55 spectrameter (KBr pellets) in the 4000–400 cm^{-1} range. The electron absorption spectra of the compounds solution (DMSO) are measured by using Perkin-Elmer Lambda 40 UV-visible spectrometer.

The relative discharge energy of Li/$SOCl_2$ battery is used to evaluate the catalytic activity of the compounds to the battery.

* Corresponding author. Tel.: +86 29 88302604; fax: +86 29 88302604.
E-mail address: jszhao@nwu.edu.cn (J. Zhao).

1381-1169/$ – see front matter © 2009 Elsevier B.V. All rights reserved.
doi:10.1016/j.molcata.2009.11.014

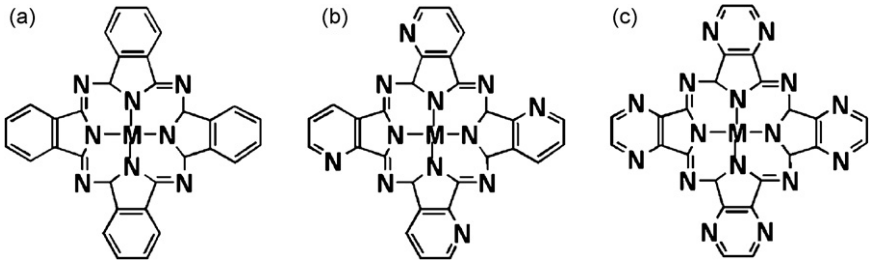

Fig. 1. The chemical structure of (a) MPc, (b) MTAP, and (c) MPTpz.

2.1. Synthesis of MPc, MTAP and MPTpz

O-phthalic anhydride, pyridine-2,3-dicarboxylic acid and 2,3-pyrazinedicarboxylic acid were obtained from Alfa Aesar Co., and all other reagents are of analytical grades and used without further purification.

MPc, MTAP, and MPTpz (M = Mn(II), Fe(II), Co(II), Ni(II) and Cu(II)) were synthesized by microwave reaction [14,27], As a route to synthesize CoTAP, a mixture of 1.50 g of pyridine-2,3-dicarboxylic acid, 6.0 g of urea, 1.38 g of $CoCl_2{\cdot}6H_2O$ and 0.06 g of $(NH_4)_2Mo_2O_7$ in 100 ml crucible is irradiated in a microwave oven at 460 W for 8 min, and then at 800 W for 8 min. After cooling to room temperature, the as-product was washed with water, acetone, methyl alcohol, 6 mol L^{-1} hydrochloric acid several times. After being vacuum dried, the purification of blue solid is done by refluxing with 150 ml of acetone, methyl alcohol, and trichloromethane respectively about 12 h. Other compounds were synthesized by the same method. The results of elemental analyses and IR spectra of the obtained products listed as follows provide evidence to the formation of proposed complexes.

MnPc: 31% yield; m.p. >300 °C; IR(KBr pellet, cm^{-1}): ν = 3421 (vs), 1611 (s), 1524 (m), 1092 (s), 941 (m), 732 (s); Anal. Cald. for $C_{32}H_{16}N_8Mn$: C, 67.73; H, 2.84; N, 19.45; Found: C, 67.34; H, 2.32; N, 20.25.

FePc: 49% yield; m.p. >300 °C; IR (KBr pellet, cm^{-1}): 1608 (s), 1518 (m), 1088 (s), 913 (m), 728 (s); Anal. Cald. for $C_{32}H_{16}N_8Mn$: C, 67.62; H, 2.84; N, 19.71; Found: C, 67.53; H, 2.73; N, 19.85.

CoPc: 53% yield; m.p. >300 °C; IR(KBr pellet, cm^{-1}): 1612 (s), 1523 (m), 1092 (s), 913 (m), 731 (s); Anal. Cald for $C_{28}H_{12}N_{12}Co$: C, 66.26; H, 2.82; N, 19.61; Found: C, 66.32; H, 2.75; N, 19.97.

NiPc: 35% yield; m.p. >300 °C; IR(KBr pellet, cm^{-1}): 1611 (s), 1507 (m), 1091 (s), 913 (m), 724 (s); Anal. Cald. for $C_{32}H_{16}N_8Ni$: C, 67.28; H, 2.82; N, 19.62; Found: C, 66.58; H, 2.51; N, 19.83.

CuPc: 67% yield; m.p. >300 °C; IR(KBr pellet, cm^{-1}): 1610 (s), 1505 (m), 1090 (s), 899 (m), 722 (s); Anal. Cald. for $C_{32}H_{16}N_8Cu$: C, 66.72; H, 2.80; N, 19.26; Found: C, 66.17; H, 2.24; N, 19.26.

MnTAP: 39% yield; m.p. >300 °C; IR(KBr pellet, cm^{-1}): 1660 (s), 1583 (s), 1524 (m), 1105 (s), 936 (m), 793 (s), 731 (s); Anal. Cald. for $C_{28}H_{12}N_{12}Mn$: C, 58.85; H, 2.12; N, 29.41; Found: C, 58.63; H, 2.23; N, 29.88.

FeTAP: 55% yield; m.p. >300 °C; IR(KBr pellet, cm^{-1}): 1664 (s), 1584 (s), 1515 (m), 1105 (s), 924 (m), 794 (s), 753 (s); Anal. Cald for $C_{28}H_{12}N_{12}Mn$: C, 58.76; H, 2.11; N, 29.37; Found: C, 58.40; H, 2.43; N, 30.02.

CoTAP: 51% yield; m.p. >300 °C; IR(KBr pellet, cm^{-1}): 1666 (s), 1585 (s), 1522 (m), 1134 (s), 923 (m), 793 (s), 745 (s); Anal. Cald. for $C_{28}H_{12}N_{12}Mn$: C, 58.45; H, 2.10; N, 29.21; Found: C, 58.23; H, 2.43; N, 29.52.

NiTAP: 53% yield; m.p. >300 °C; IR(KBr pellet, cm^{-1}): 1641 (s), 1579 (s), 1531 (m), 1087 (s), 931 (m), 788 (s), 744 (s); Anal. Cald. for $C_{28}H_{12}N_{12}Ni$: C, 58.47; H, 2.10; N, 29.22; Found: C, 58.31; H, 2.43; N, 29.45.

CuTAP: 69% yield; m.p. >300 °C; IR(KBr pellet, cm^{-1}): 1673 (s), 1580 (s), 1506 (m), 1096 (s), 909 (m), 756 (s), 737 (s); Anal. Cald. for $C_{28}H_{12}N_{12}Cu$: C, 57.98; H, 2.09; N, 28.98; Found: C, 57.61; H, 2.31; N, 29.24.

MnPTpz: 45% yield; m.p. >300 °C; IR(KBr pellet, cm^{-1}): 1624 (s), 1525 (m), 1166 (s), 911 (m), 756 (s); Anal. Cald for $C_{24}H_8N_{16}Mn$: C, 50.10; H, 1.40; N, 38.95; Found: C, 49.87; H, 1.56; N, 39.17.

FePTpz: 59% yield; m.p. >300 °C; IR(KBr pellet, cm^{-1}): 1628 (s), 1527 (m), 1111 (s), 935 (m), 755 (s); Anal. Cald. for $C_{24}H_8N_{16}Fe$: C, 50.02; H, 1.40; N, 38.89; Found: C, 49.73; H, 1.58; N, 39.12.

CoPTpz: 54% yield; m.p. >300 °C; IR(KBr pellet, cm^{-1}): 1631 (s), 1516 (m), 1120 (s), 934 (m), 756 (s); Anal. Cald. for $C_{24}H_8N_{16}Fe$: C, 49.75; H, 1.39; N, 38.68; Found: C, 49.42; H, 1.62; N, 38.95.

NiPTpz: 57% yield; m.p. >300 °C; IR(KBr pellet, cm^{-1}): 1639 (s), 1531 (m), 1121 (s), 933 (m), 754 (s); Anal. Cald. for $C_{24}H_8N_{16}Ni$: C, 49.77; H, 1.39; N, 38.70; Found: C, 49.55; H, 1.45; N, 39.03.

CuPTpz: 73% yield; m.p. >300 °C; IR(KBr pellet, cm^{-1}): 1613 (s), 1526 (m), 1144 (s), 916 (m), 754 (s); Anal. Cald for $C_{24}H_8N_{16}Cu$: C, 49.36; H, 1.38; N, 38.38; Found: C, 49.16; H, 1.50; N, 38.52.

2.2. Electrochemistry

The electrochemical measurements were carried out in specially designed test cells. The compartment of the cells is made from PTFE material. The preparation of carbon cathode started from a mixture of 92 wt.% acetylene black and 8 wt.% Teflon binder. Then the pastes were formed by adding water and iso-propyl-alcohol into the mixture. Subsequently, the mixture pastes were dried at 120 °C for 4 h.These carbon electrodes were used as cathode with the apparent (exposed) area of 1 cm^2, and lithium foils were used as the counter electrodes. A 1.47 mol L^{-1} $LiAlCl_4$–$SOCl_2$ solution containing 5×10^{-3} mol L^{-1} MPc, MTAP and MPTpz (M = Mn^{2+}, Fe^{2+}, Co^{2+}, Ni^{2+} and Cu^{2+}) compounds were used. The discharge tests for the lithium-thioyl chloride batteries were evaluated at a constant resistance 40 Ω, and were stopped until the voltage reached 2 V. ALL the experiments were conducted in a glove box under an argon atmosphere (MBRAUN, MB-BL-01).

3. Results and discussion

Fig. 2 shows the discharge curves of Li/$SOCl_2$ battery catalyzed by MPc derivatives. It shows that the catalytic activity of MPc is different, depending on the central metal ions (as shown in Fig. 2a). In comparison to the same central metal ions, the catalytic activity of MTAP is much higher than that of MPc (as shown in Fig. 2b), while the catalytic activity of MPTpz is relative low and almost independent of the central metal ions (as shown in Fig. 2c).

The discharge energy of Li/$SOCl_2$ battery is

$$E = \int P\,dt = 1/Re \sum U^2 \Delta t \quad (1)$$

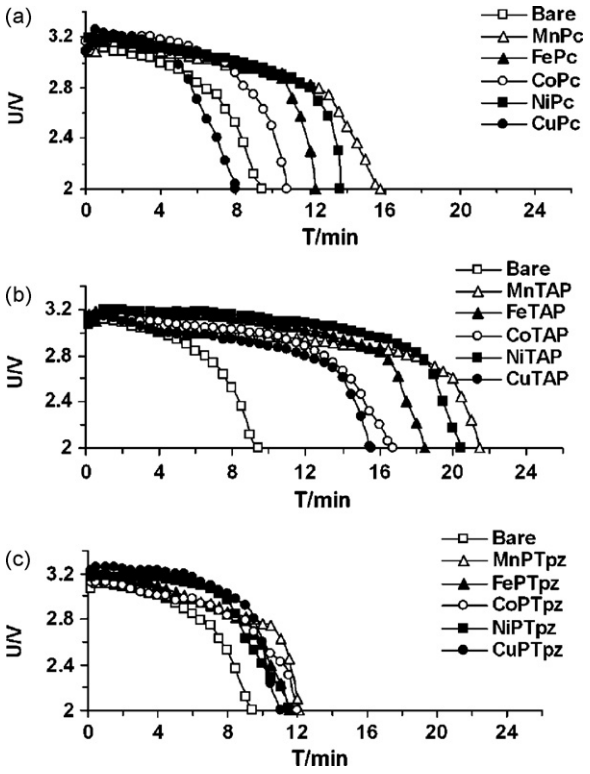

Fig. 2. The discharge curves of Li/$SOCl_2$ battery ($LiAlCl_4$–$SOCl_2$ electrolyte, 1.47 mol L^{-1}; constant discharge resistance, 40 Ω; apparent electrode area, 1 cm^2). (a) Electrolyte solution containing MPc (M = Mn^{2+}, Fe^{2+}, Co^{2+}, Ni^{2+} and Cu^{2+}, respectively), 5×10^{-3} Mol L^{-1}. (b) Electrolyte solution containing MTAP, 5×10^{-3} Mol L^{-1}. (c) Electrolyte solution containing MPTpz, 5×10^{-3} Mol L^{-1}.

The relative energy (X) of the battery is:

$$X(\%) = \frac{E}{E_0} \times 100 \quad (2)$$

where P stands for the power of the battery, R_e stands for the external resistance, U stands for the discharge voltage, t stands for the discharged time, E stands for the energy of the battery, E_0 stands for the energy of the battery in the absence of complexes.

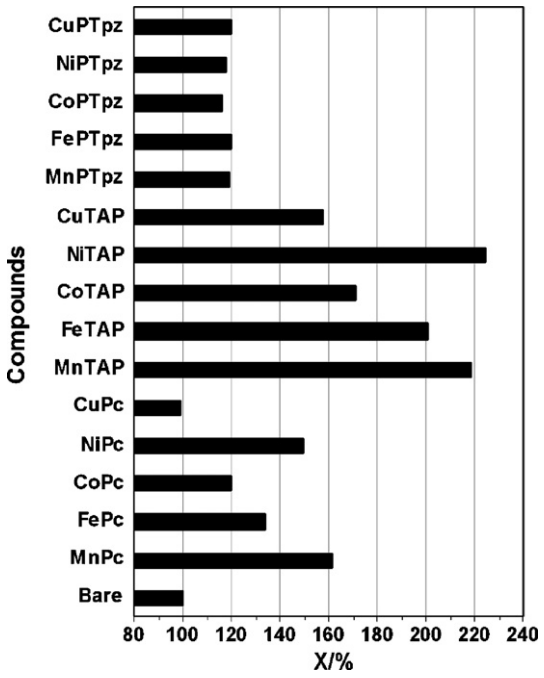

Fig. 3. The compounds and the relative energy of Li/$SOCl_2$ battery.

The relative energy (X) of lithium battery reflects the catalytic activity of ML clearly (as shown in Fig. 3). The discharge energy of Li/$SOCl_2$ battery catalyzed by MPc (M = Mn^{2+}, Fe^{2+}, Co^{2+}, and Ni^{2+}) depends on the central metal ion, which is approximately 20–61% higher than that of Li/$SOCl_2$ battery in the absence of complexes. The discharge energy of Li/$SOCl_2$ battery catalyzed by MTAP is 60–123% higher than that of Li/$SOCl_2$ battery in the absence of complexes. It is very interesting to find that to the same metal ion of the compounds, the discharge energy of Li/$SOCl_2$ battery catalyzed by MTAP is approximately 60% higher than that by MPc. The discharge energy of Li/$SOCl_2$ battery in which $SOCl_2$ contains

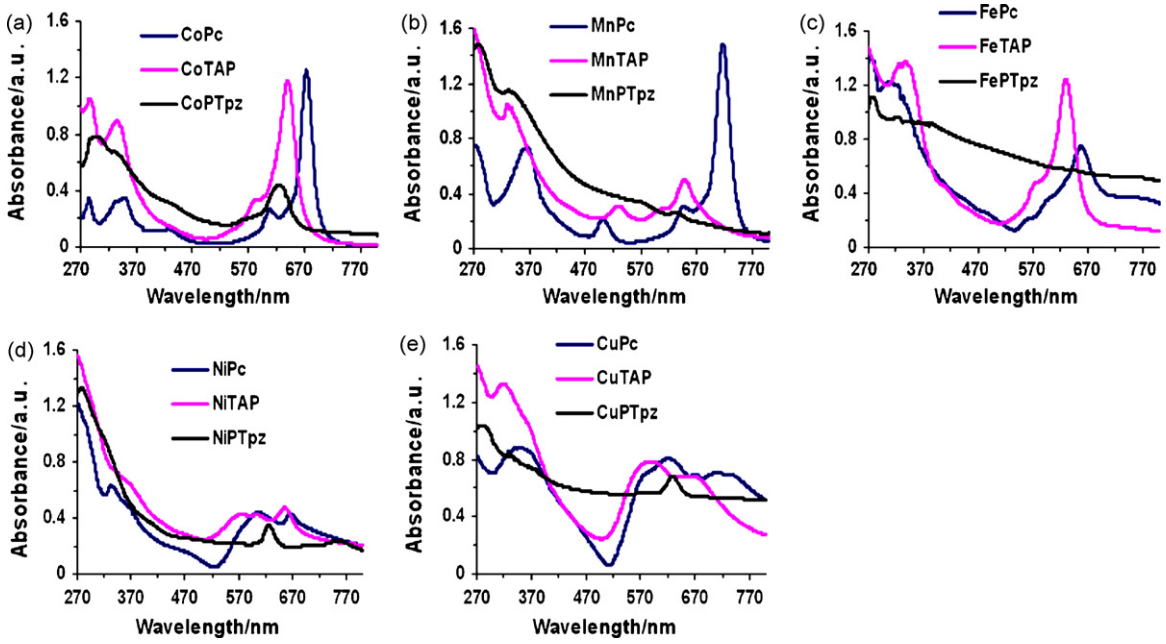

Fig. 4. UV–vis spectra of ML (M = Co^{2+}, Mn^{2+}, Fe^{2+}, Ni^{2+} and Cu^{2+}, L = Pc, TAP and PTpz, respectively), 1×10^{-4} mol L^{-1}(DMSO).

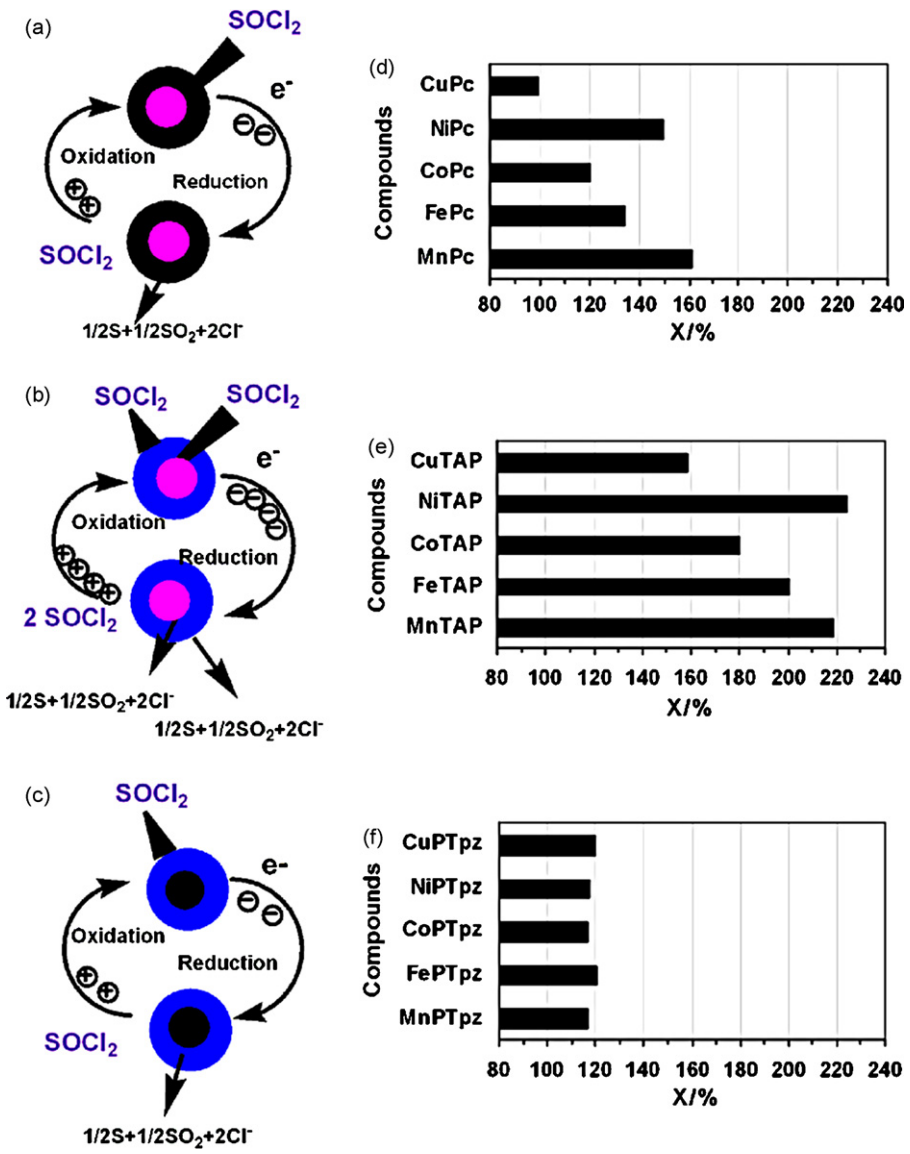

Fig. 5. The DASM and the relative energy of Li/$SOCl_2$ battery. Pink small circle, central metal ion active site; black small circle, central metal ion inactive site; blue big circle, ligand active site; black big circle, ligand inactive site.

MPTpz (M = Mn^{2+}, Fe^{2+}, Co^{2+}, Ni^{2+} and Cu^{2+}) increases approximately 17–19% higher than that of the battery in the absence of complexes, and almost independent of central metal ions.

The reduction of $SOCl_2$ catalyzed by MPc is an electron transfer process, which is accomplished by the external electrons of MPc. The intensity of UV–vis spectra exhibits the transfer process of external electrons of MPc derivatives. The UV–vis spectra of MPc, MTAP and MPTpz are investigated to show the electron transitions between highest occupied molecular orbital (HOMO) and the lowest orbital (LUMO) of the metal phthalocyanines (Fig. 4). To CoPc, the strongest band in the wavelength region of 580–710 nm ascribed to the π–π transition centered on the macrocycle of CoPc molecules, is the Q band. The UV–vis spectrum of CoPc shows two peaks of Q band at 596 and 672 nm, representing the characteristic bands of dimer and monomer of CoPc, respectively. The intensity of the dimer is much lower than that of the monomer. The activity of the Q band is mainly attributed to the monomer because the dimer has little activity. Another band in the wavelength region of 280–360 nm due to the backbone of the phthalocyanine ring, is the B band. There are a relatively strong Q band and a weak B band existing in the electron absorbance of CoPc. The Q band of CoTAP is within the range of 550–670 nm and two peaks of Q band are at 577 and 638 nm, representing the characteristic bands of dimer and monomer of CoTAP, respectively. The B band of CoTAP is within the region of 270–370 nm. Compared to CoPc, the B band absorbance of CoTAP is much higher than that of CoPc, whereas the Q band absorbance of CoTAP and the intensity of the dimer and the monomer of CoTAP are similar to that of CoPc. The B band and Q band of CoPTpz are in the wavelength region of 270–360 nm and 580–650 nm, respectively. There exists a relative strong and broaden B band but no significant Q band in the electron absorbance of CoPTpz (as shown in Fig. 4a). The B bands and Q bands of the electron absorbance of other metal phthalocyanines MPc (M = Mn^{2+}, Fe^{2+}, and Ni^{2+}), MTAP and MPTpz, have similarity with that of CoL, while a little differences existed among them (as shown in Fig. 4b–e).

The mechanism of the reduction of $SOCl_2$ by MPc derivatives has been demonstrated in many papers [15–20]. Bernstein has shown the formation of the adduct MPc·$SOCl_2$ is the key step in this catalytic reduction reaction [15].

On the basis of the results and the mechanism of the catalytic reduction by metal phthalocyanine demonstrated by Bernstein, a

simple kinetic model, named Double Active Site Model (DASM) is proposed to show the process of the reduction of $SOCl_2$ catalyzed by ML (ML = MPc, MTAP and MPTpz).

(1) $SOCl_2$ is adsorbed by ML, and an adduct ML·$SOCl_2$ is formed [15]. As a molecular catalyst, the ligand (L) and the central metal ion (M) of ML are potential catalytic active sites. The adduct of ML·$SOCl_2$ can be formed through two ways: the coordination between the O atom of $SOCl_2$ and M^{2+} of ML, and the injection of the N atoms of L in the holes of $SOCl_2$.

$$ML + SOCl_2 \xrightarrow{k_1} ML \cdot SOCl_2 \quad (3)$$

$$ML + SOCl_2 \xrightarrow{k_2} ML \cdot SOCl_2 \quad (4)$$

where k_1 is the rate constant for formation of ML·$SOCl_2$ through the former way $SOCl_2$, and k_2 is the rate constant for formation of ML·$SOCl_2$ through the latter one.

In the strong ligand field, due to Jahn–Teller effect, Cu^{2+} is square coordinate configuration, and the ligand L occupy the four coordinate sites, the coordinate bond between O atom of $SOCl_2$ and Cu^{2+} of ML cannot form, therefore CuL has only one potential catalytic activity site.

(2) The adduct ML·$SOCl_2$ accepts the electrons. S, SO_2 and Cl^- leave, and ML is returned (Fig. 4).

$$ML \cdot SOCl_2 + 2e \xrightarrow{k_3} ML + 1/2S + 1/2SO_2 + Cl^- \quad (5)$$

where k_3 is the rate constant for the reduction of ML·$SOCl_2$.

The formation of the adduct ML·$SOCl_2$ is the rate-controlling step [15]. The overall catalytic activity of the compounds to the reduction of $SOCl_2$ depends on both the competitive and cooperative process of the two ways of the formation of the ML·$SOCl_2$.

MPc has relative strong electron absorbance in Q band and weak in B band, MPc has only one catalytic active site, that is M [28], therefore the catalytic activity of MPc to lithium battery depends on the central metal ions (as shown in Fig. 5a and d). In contrast, MPTpz has relative strong electron absorbance in B band and weak in Q band, MPTpz has only one catalytic active site, that is L of MPTpz, therefore the catalytic activity of MPTpz to lithium battery is independent of the central metal ions (as shown in Fig. 5c and f). The feature of MTAP exhibits strong electron absorbance spectra both in Q band and B band, and MTAP has two catalytic activity sites which are M and L, showing excellent catalytic activity to lithium battery (as shown in Fig. 5b and e).

4. Conclusions

N atoms in the backbone of MPc derivatives strongly affect their catalytic sites and their catalytic activity to Li/$SOCl_2$ battery. MPc has only one catalytic active site on the central metal ion of the compounds. The catalytic activity of MPc to lithium battery depends on the central metal ions of the compounds. CuPc is inactive due to Jahn–Teller effects. In contrast, MPTpz has only one catalytic active site on the ring of the compounds. The catalytic activity of MPTpz to lithium battery remains the same level, independent on the central metal ions of the compounds. MTAP (M = Mn^{2+}, Fe^{2+}, Co^{2+} and Ni^{2+}) have two catalytic active sites with relative high activity. MnTAP and NiTAP are the two most effective catalysts to the battery among the test compounds. The energy of Li/$SOCl_2$ battery whose electrolyte contains MnTAP and NiTAP improves 119%, 123%, respectively.

Acknowledgements

We acknowledge financial support from Chinese nature science foundation (Nos. 20671076 and 20971104), the Ph.D. Program Foundation of Ministry of Education of China (No. 200806970008) and Foundation of National Science and Technology Pillar Program of China (No. 2007BAB17B02), and the Doctorate Foundation of Northwestern Polytechnical University.

References

[1] E.M. Bauer, M.P. Donzello, C. Ercolani, E. Masetti, S. Panero, G. Ricciardi, A. Rosa, A. Chiesi-Villa, C. Rizzoli, Inorg. Chem. 42 (2003) 283–293.
[2] P.Y. Reddy, L. Giribabu, C. Lyness, H.J. Snaith, C. Vijaykumar, M. Chandrasekharam, M. Lakshmikantam, J. Yum, K. Kalyanasundaram, M. Gratzel, M.K. Nazeeruddin, Angew. Chem. Int. Ed. 46 (2007) 373–376.
[3] A. Muranaka, M. Okuda, N. Kobayashi, K. Somers, A. Ceulemans, J. Am. Chem. Soc. 126 (2004) 4596–4604.
[4] Q.M. Zhang, H.F. Li, M. Poh, F. Xia, Z.Y. Chmg, H.S. Xu, C. Huang, Nature 419 (2002) 284–287.
[5] E. Barrena, X.N. Zhang, B.N. Mbenkum, T. Lohmueller, T.N. Krauss, M. Kelsch, P.A. Aken, J.P. Spatz, H. Dosch, ChemPhysChem 9 (2008) 1114–1116.
[6] J.F. Ma, Y.N. Liu, P. Zhang, J. Wang, Electrochem. Commun. 10 (2008) 100–102.
[7] M.R. Nabid, R. Sedghi, P.R. Jamaat, N. Safari, A.A. Entezami, Appl. Catal. A 328 (2007) 52–57.
[8] A. Sorokin, J.-L. Séris, B. Meunier, Science 268 (1995) 1163–1166.
[9] F.C. Moraes, M.F. Cabral, S.A.S. Machado, L.H. Mascaro, Electroanalysis 20 (8) (2008) 851–857.
[10] P. Kluson, M. Drobek, T. Strasak, J. Krysa, M. Karaskova, J. Rakusan, J. Mol. Catal. A 272 (2007) 213–219.
[11] D. Carmier, C. Vix-Guterl, J. Lahaye, Carbon 39 (2001) 2181–2196.
[12] D. Carmier, C. Vix-Guterl, J. Lahaye, Carbon 39 (2001) 2187–2193.
[13] G.T.K. Fey, M. Hsieh, Y.C. Chang, J. Power Sources 97–98 (2001) 606–609.
[14] Z.W. Xu, J.S. Zhao, H.J. Li, K.Z. Li, Z.Y. Cao, J.H. Lu, J. Power Sources 194 (2009) 1081–1084.
[15] P.A. Bernstain, A.B.P. Lever, Inorg. Chem. 29 (1990) 608–616.
[16] K.M. Abraham, M. Alamgir, E.B. Willstaedt, W.P. Kilroy, J. Power Sources 45 (3) (1993) 343–435.
[17] S.B. Lee, S.I. Pyun, E.J. Lee, Electrochim. Acta 47 (2001) 855–864.
[18] W.S. Kima, Y.K. Choi, Appl. Catal. A 252 (2003) 163–172.
[19] Y.K. Choi, W.S. Kim, K. Chung, M.W. Chung, H.P. Nam, Microchem. J 65 (2000) 3–15.
[20] W.S. Kim, W.J. Sim, K. Chung, Y.E. Sung, Y.K. Choi, J. Power Sources 45 (3) (1993) 343–352.
[21] A.R. Silva, M. Martins, M.M.A. Freitas, A. Valente, C. Freire, B. Castro, J.L. Figueiredo, Micropor. Mesopor. Mater. 55 (2002) 275–284.
[22] M. Stantney, W. ham, Chem. Rev. 104 (2004) 4271–4301.
[23] M. Pomerantz, A. Aviram, R.A. McCorkle, L. Li, A.G. Schrott, Science 255 (1992) 1115–1118.
[24] C.Y. Tsai, S.P. Chen, T.C. Wen, Chem. Phys. 240 (1999) 191–196.
[25] B.H. Lee, J.Y. Jaung, S.C. Jang, S.C. Yi, Dyes Pigments 65 (2005) 159–167.
[26] D. Dini, M. Hanack, H.J. Egelhaaf, J.C. Sancho-Garcĭa, J. Cornil, J. Phys. Chem. B 109 (2005) 5425–5432.
[27] A. Shaabani, R. Maleki-Moghaddam, A. Maleki, A.H. Rezayan, Dyes Pigments 74 (2007) 279–282.
[28] G.J. Yang, J.J. Xu, K. Wang, H.Y. Chen, Electroanalysis 18 (3) (2006) 282–290.